

Radial microstructure and optical properties of a porous silicon layer by pulse anodic etching*

Long Yongfu(龙永福)[†]

Department of Physics and Electronics, Hunan University of Arts and Science, Changde 415000, China

Abstract: This paper investigates the radial refractive index and optical and physical thicknesses of porous silicon (PS) layers prepared by pulse etching by means of reflectance spectroscopy, photoluminescence spectroscopy and scanning electron microscopy (SEM). The relationship between the radial refractive index and optical thickness of the PS sample and the position away from the etched centre along the radial direction has been analyzed in detail. With the position farther away from the etched centre, the SEM image shows that the physical thickness of the PS sample decreases slowly, whereas intensely decreases from 2.48 to 1.72 μm near the edge at a distance of 58 μm . Moreover, the radial refractive index increases, indicating that the porosity becomes smaller. Meanwhile, the reflectance spectra exhibit the less intense interference oscillations, which mean that the uniformity and interface smoothness of the PS layers become worse, and the envelope curves of photoluminescence spectra exhibit a trend of blue-shift, indicating a reduction in nanocrystal dimensions. The PS micro-cavity is prepared to study the radial optical properties of the PS layer, and the results verify that the uniformity and smoothness of the PS layer in the centre are better than those at the edge.

Key words: porous silicon; radial microstructure; optical thickness; photoluminescence

DOI: 10.1088/1674-4926/32/4/043003

EEACC: 2520

1. Introduction

The discovery of strong visible light emission from porous silicon (PS)^[1] has awakened interest in a wide variety of applications, including optoelectronics, chemical sensing and optical components. Some properties of the PS layer, such as the refractive index, porosity, physical and optical thickness and pore diameter, are strongly dependent on the etched parameters^[2], including HF concentration, current density, temperature^[3], and Si wafer type and resistivity. In 1995, Pavese *et al.*^[4] first reported porous silicon micro-cavities (PSMs) by stacking high and low refractive index layers periodically, resulting in the full width at half maxima (FWHMs) of 15 nm. In 2002, Reece *et al.*^[5] fabricated the high-quality PS optical microcavities at $-22.5\text{ }^\circ\text{C}$ operating in the near infrared range with a line-width of 0.63 nm. However, the theoretical simulation^[5] of PSM predicts that even a resonance line-width of 0.1 nm can be fabricated. The different FWHMs of PSMs are fabricated by the above groups, indicating that the microcavity quality depends on fabricated conditions and the optical parameters of PS layers. In general, the quality of the PSM is decided by the uniformity and interface smoothness of the PS layers^[6]. In order to improve the quality of the PSM, the parameters, such as the refractive index (n), physical thickness (d), optical thickness (nd), uniformity and interface smoothness of the PS layers, must be accurately controlled to maintain a reproducible process with very good uniformity and interface smoothness of the PS layers.

Previous researches^[2, 3] have concentrated on the effects of anodic parameters on the microstructures and optical prop-

erties of the whole PS layer. Several methods, including pulse etching^[7], the positive and negative pulse etching method^[8], etching with an ultrasonic wave^[9] and decreasing the etching temperature^[3, 5], have been put forward to improve the quality of the PS layers, resulting in a lot of valuable experimental results. However, these researches were mostly carried out without considering the radial position, and the relationship between the radial microstructures and the optical properties of the PS layers and the radial position has scarcely been studied. In 2009, Long *et al.*^[10] first investigated the relationship between the downward uniformity and interface smoothness of the PS layer and etching depth, and obtained a trend in the increase in porosity or decrease in refractive index along the vertical direction. Another paper^[11] reported on the radial microstructures and optical properties of the PS layer.

In this work, the microstructures and optical properties of a PS sample are investigated at different positions along the radial direction, and the refractive index and optical thickness of the PS sample are determined with high accuracy in the spectra range.

2. Experiment

A (100) oriented, highly doped P-type silicon wafer with resistivity of 0.007–0.01 $\Omega\text{-cm}$ was cut into pieces, and the diameter of each being 14 mm was etched. The etching electrolyte was composed of HF (40%), H₂O and ethanol with the volume proportions of 1 : 2 : 1. The PS sample was prepared in the dark at an electrolyte temperature of $-10\text{ }^\circ\text{C}$ with a current density of 140 mA/cm², repetition rate of 200 Hz, duty cycle

* Project supported by the National Natural Science Foundation of China, and the Hunan Provincial Natural Science Foundation of China, and the Fund of the 12th Five-Year Plan for Key Construction Academic Subject (Optics) of Hunan Province, China.

[†] Corresponding author. Email: yongfulong@163.com

Received 25 October 2010, revised manuscript received 6 December 2010

© 2011 Chinese Institute of Electronics

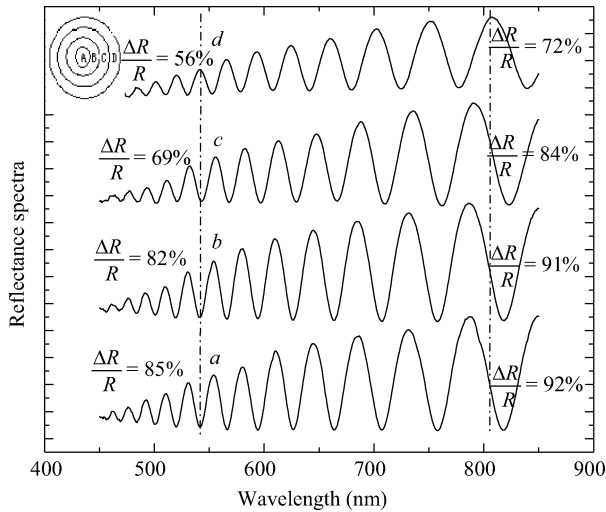


Fig. 1. Reflectance spectra of PS sample in positions A, B, C and D, corresponding to curves (a), (b), (c) and (d), respectively.

of 0.5 and etching time of 1 min, resulting in sponge-like PS structures of $\sim 2.80 \mu\text{m}$ thickness in the etched centre.

In this work, the pulse current source was generated by a TekVISA AFG3101 signal generator. The physical thickness of the PS sample was measured with a Philips XL 30 FEG field emission scanning electron microscope (SEM). According to the peaks of the measured reflectance spectra and Bragg formula, the optical thickness of the PS sample can be calculated. The excitation source for the reflectance spectra measurements was a 250 W tungsten halogen lamp; signals were amplified by standard lock-in techniques, and then detected by a photomultiplier. The PL spectra were excited by the 405 nm light beam from a semiconductor laser with a power of 5 mW and a spot size of about 1 mm^2 on the sample. The PL measurement was carried out by the same detection apparatus as used for the reflectance measurement. The refractive index was obtained as the ratio of the optical thickness resulting from the highly accurate reflectance spectra measured at a wavelength of around 700 nm to the physical thickness d obtained from the cross-section SEM measurement.

Four positions were measured on prepared samples along the radial direction from the etched centre to the edge, corresponding to positions A, B, C and D, with an adjacent distance of 2 mm, respectively.

3. Results

The reflectance spectra of PS samples in positions A, B, C and D are shown in Fig. 1 as curves (a), (b), (c) and (d), respectively. As shown in the figure, clear intensity oscillations appear over the wavelength range of 500–850 nm, resulting from the optical interferences between the light beams reflected from the top and bottom surface of the PS layers. The reflectance spectra of the four positions exhibit obvious oscillations at around the wavelength of 810 nm, but the oscillation amplitude (ΔR) decreases with wavelength λ . The decreasing rates are position dependent: for position D away from the etched centre of 6 mm, it almost disappears for wavelengths less than 500 nm, but for position A in the etched centre, it

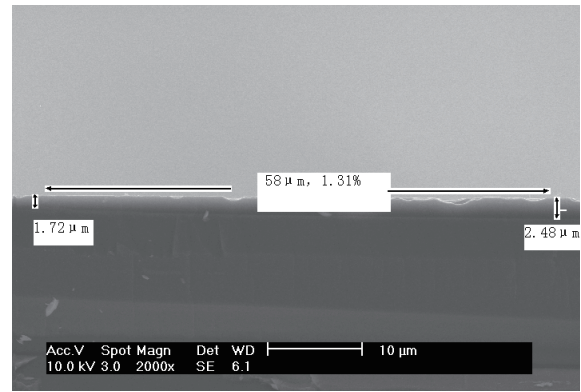


Fig. 2. Cross-sectional SEM images of the PS sample from the centre to the edge in the radial distance of $58 \mu\text{m}$ near the edge, corresponding to the position from right to left.

remains almost unchanged over the whole wavelength range in the figure. At the long-wavelength of 810 nm, the ratios ($\Delta R/R$) of the oscillation amplitude (ΔR) to the maximum reflectance intensity (R) are 92%, 91%, 84% and 72%, and at the short-wavelength of 540 nm, the ratios ($\Delta R/R$) only are 85%, 82%, 69% and 56%, respectively, for positions A, B, C and D, as shown in Fig. 1, indicating that the ratio ($\Delta R/R$) decreases with position far away from the etched centre. In general, the interference-intensity^[6] of the mono-layer depends on the uniformity of the layer and the smoothness of the top and bottom interfaces. Therefore, the present experimental results show that position A in the etched centre is the most uniform with the smoothest surface and interface, and with position farther away from the etched centre, the worse uniformity and rougher interface of the layer will be formed.

According to the measurement of the interference fringes in the reflectance spectrum of the PS layer, the optical thickness (nd) of the PS layer can be calculated by interference equation^[2,12],

$$nd = \frac{\lambda_{r+1}\lambda_r}{2(\lambda_{r+1} - \lambda_r)}, \tag{1}$$

where λ_r is the wavelength of the r -th fringe. The optical thicknesses of the PS sample in positions A, B, C and D are obtained as 5480, 5460, 5450 and 5390 nm, respectively, at a wavelength of around 700 nm, indicating a trend that the optical thickness decreases with position away from the etched centre. Within the experimental error, it can be considered that four positions had the same optical thicknesses. Furthermore, detailed investigation into the SEM image shows that the physical thickness of the PS sample decreases slowly from 2.82 down to $2.70 \mu\text{m}$ as the position from the etched centre to the edge at a distance of 6 mm. The SEM images of the cross-section of the PS sample from the etched centre to the edge in a short distance near the edge, corresponding to the position from right to left, is presented in Fig. 2. It can be seen that the physical thickness intensely decreases from 2.48 to $1.72 \mu\text{m}$ in the radial distance of $58 \mu\text{m}$, corresponding to an average variation ratio (the variation in the physical thickness per unit radial distance) of $13.1 \text{ nm}/\mu\text{m}$. The results showed that the physical thickness intensely decreases near the edge along the radial direction.

Combining the physical thickness measurements from

Table 1. Optical parameters of four positions along the radial direction.

Parameter	Position			
	A	B	C	D
Optical thickness (nm)	5480	5460	5450	5390
Physical thickness (μm)	2.82	2.82	2.78	2.70
Refractive index	1.94	1.94	1.96	2.0

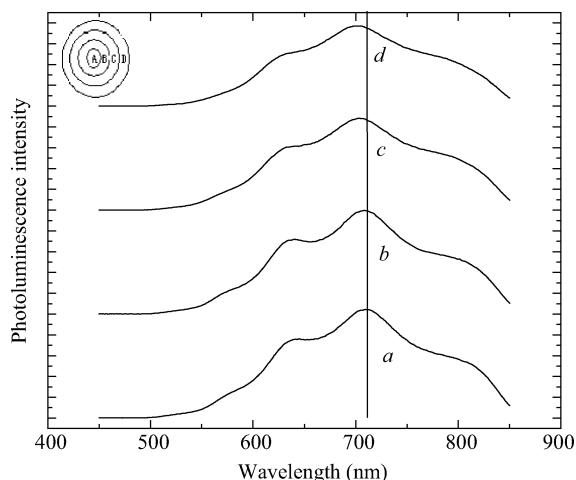


Fig. 3. PL spectra of the PS sample in positions A, B, C and D, corresponding to curves (a), (b), (c) and (d), respectively.

SEM with the optical thickness determination from the oscillations of the reflectance spectra, the refractive indices were calculated to be 1.94, 1.94, 1.96 and 2.0 for positions A, B, C and D, respectively. Furthermore, the detailed investigation of the SEM images (not shown in the present paper) shows that the average diameter of the PS holes decreases from 25 nm down to 15 nm along the radial direction from the etched centre to the edge. Table 1 lists the relationship between the optical thickness, refractive index and position along the radial direction. The obtained refractive index exhibits a trend of increase with position far away from the etched centre.

The above experimental results show that the rate of the radial optical thickness of the PS layer is almost constant but the etching rate of the physical thickness decreasing along the radial direction demonstrates that under the same etching conditions, the position nearer the etched centre leads to a more uniform PS layer with a smoother interface, higher porosity and smaller refractive index along the radial direction, contrarily, the worse quality of PS layer will be formed with the position farther away from the etched centre, especially near the edge.

PL spectra of the PS sample in positions A, B, C and D are shown in Fig. 3 as curves (a), (b), (c) and (d), respectively. The peaks of the envelope curves of the PL spectra in Fig. 3 exhibit a trend of blue-shift that may in part be explained by the reduction in nanocrystal dimensions^[2, 13], the decrease in porosity or the increase in refractive index with position far away from the etched centre. The experimental results are in agreement with the above SEM analysis.

In order to study further the uniformity and interface smoothness of the PS layers along the radial direction, the PSM was fabricated at 5 °C, structurally, corresponding to the designed wavelength of λ ($\lambda = 660$ nm). The PSM was com-

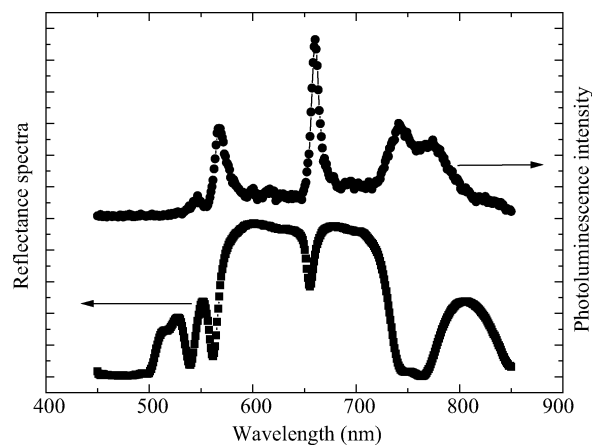


Fig. 4. Reflectance and PL spectra experimentally measured from the PSM in the etched centre.

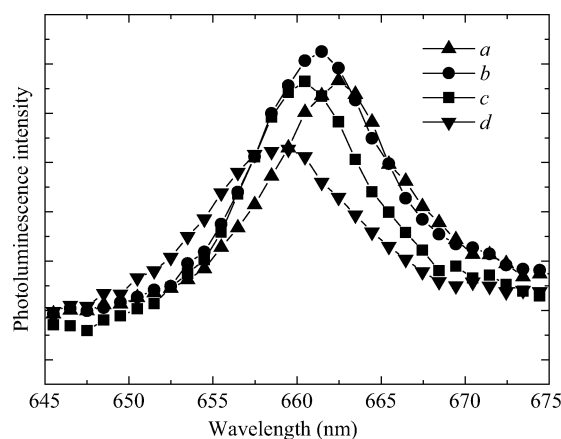


Fig. 5. PL spectra experimentally measured from the PSM in positions A, B, C and D along the radial direction from the centre to the edge, with the adjacent distance of 2 mm, corresponding to curves (a), (b), (c) and (d), respectively.

posed of an active PS layer (ACL) of 82% porosity [index of refractive $n = 1.30$ (Ref. [3])] with an optical thickness of $\lambda/4$ sandwiched between two distributed Bragg-reflectors (DBRs) made up of 6 pairs of alternating high and low refractive index layers with porosity of 72% [$n = 1.45$ (Ref. [3])] and 51% [$n = 2.10$ (Ref. [3])], respectively, with the same optical thickness of $\lambda/2$. All of the layers of PSM were fabricated by controlling the current density and etching time, using the above-mentioned fabricated conditions, methods and experimental setups.

Two measurements were performed to study the optical properties of the PS film along the radial direction: (1) PSM normal-incidence reflectance and photoluminescence emission; and (2) comparative PL spectra of PSM along the radial direction from the etched centre to the edge.

Figure 4 shows the reflectance and PL spectra of the PSM sample. The peak of reflectance and PL spectra is located at 663 nm with the FWHM of 9 nm in position A, namely, the etched centre. In general, the quality (Q) fact of the microcavity, which is given by the ratio ($\lambda/\Delta\lambda$) of the mode position and the width, is equal to 74. In Fig. 5, the PL spectra of the PSM in positions A, B, C and D are shown as curves (a), (b), (c) and (d), respectively. As shown in the figure, the PL peaks

are 663, 662, 661 and 659 nm, corresponding to the FWHMs of 9, 10, 10 and 12 nm, the quality (Q) fact of 74, 66, 66 and 55, respectively. The above results show that the PL peaks of the PSM sample blue-shift with position away from the centre to the edge. Narrow PL peaks with FWHMs of 9–12 nm positioned in the wavelength range of 659–663 nm were achieved from the PSM fabricated by electrochemically etching silicon. In general, the FWHF of the resonant PL peaks from the PSM can be considered a reflection of the PS film quality. The above results verified that the quality of the PSM became worse with position away from the etched centre, and also found that the PL peaks of the PSM show an almost blue-shift trend from the position A in the centre of the PSM to B, C and D along the radial direction. The optical property analysis of both the PS single layer and the PSM indicates that nearer the etched centre is greater uniformity with a smoother interface of the PS layers.

4. Discussions

The above experimental results can be explained by the following mechanism. Firstly, according to the diffusion law, the rate of diffusion of reaction products away from the pores increases and HF into the holes decreases along the radial direction from the edge to the etched centre. The HF concentration in the holes in the etched centre is lower than that at the edge, resulting in the F^- concentration decreasing along the radial direction, which facilitates lateral erosion of the micro-pore walls^[2] of the etched centre, resulting in larger pore diameters or porosity. Secondly, in the electrochemical etching process, the reaction produces hydrogen bubbles in the PS layer and increases along the radial direction from the edge to the centre, which forms the gradients of concentrations and leads to the lowest HF and highest hydrogen concentration in the etched centre, thus the resistance in the etching process goes up along the radial direction. This phenomenon was also observed in the previous paper^[7]. In the period of etching, using the constant current density results in the constant vertical etching effectiveness. At the same time, because of increasing resistance of the etching electrolyte^[7], resulting in the electric field in the PS layer increasing from the edge to the centre along the radial direction, this can excite a lot of holes in the side walls Si atoms of micropores and form a gradient of holes and generate the highest concentration of holes at the etched centre, the F^- facilitates etching of the side wall Si atoms of the etched centre to form Si–F bonds, thus also strengthening the lateral etching ability, resulting in an increase in porosity or a decrease in the refractive index. The results demonstrate that the uniformity of the PS layer becomes worse along the radial direction from the centre to the edge, namely, the refractive index increases and the porosity decreases, which is consistent with the above experimental results.

5. Conclusion

In summary, the dependence of the uniformity and optical properties on the position in the radial direction has been investigated. The experimental results demonstrated that under otherwise constant etching conditions, nearer the etched centre, leading to thicker physical and optical thicknesses, higher porosity and lower refractive index, more uniform PS layer with smoother interface along the radial direction.

Acknowledgements

The authors thank Prof Hou X. Y. and Prof Ding X. M. for their fruitful instructions and discussions, and Dr Ge J. for assistance in experiments.

References

- [1] Canham L T. Silicon quantum wire array fabrication by electrochemical and chemical dissolution of wafers. *Appl Phys Lett*, 1990, 57: 1046
- [2] Bisi O, Ossicini S, Pavese L. Porous silicon: a quantum sponge structure for silicon based optoelectronics. *Surf Sci Rep*, 2000, 38: 1
- [3] Long Yongfu, Ge Jin, Ding Xunmin, et al. Temperature: a critical parameter affecting the optical properties of porous silicon. *Journal of Semiconductors*, 2009, 30: 063002
- [4] Pavese L, Mazzoleni C, Tredicucci A, et al. Controlled photon emission in porous silicon microcavities. *Appl Phys Lett*, 1995, 67: 3280
- [5] Reece P J, Lérondel G, Zheng W H, et al. Optical microcavities with subnanometer linewidths based on porous silicon. *Appl Phys Lett*, 2002, 81: 4895
- [6] Xu S H, Xiong Z H, Gu L L, et al. Photon confinement in one-dimensional photonic quantum-well structures of nanoporous silicon. *Solid State Commun*, 2003, 126: 125
- [7] Hou X Y, Fan H L, Xu L, et al. Pulsed anodic etching: an effective method of preparing light-emitting porous silicon. *Appl Phys Lett*, 1996, 68: 2323
- [8] Ge J, Yin W J, Long Y F, et al. Positive and negative pulse etching method of porous silicon fabrication. *Chin Phys Lett*, 2007, 24: 1361
- [9] Liu Y, Xiong Z H, Liu Y, et al. A novel method of fabricating porous silicon material: ultrasonically enhanced anodic electrochemical etching. *Solid State Commun*, 2003, 127: 583
- [10] Long Yongfu, Ge Jin. Downward uniformity and optical properties of porous silicon layers. *Journal of Semiconductors*, 2009, 30: 052003
- [11] Long Y F, Ge J. Radial microstructure and optical properties of porous silicon layer. *INEC: 2010 3rd International Nanoelectronics Conference*, 2010, 1/2: 1244
- [12] Strashnikova M I. On measurements of the refractive index dispersion in porous silicon. *Optics and Spectroscopy*, 2002, 93: 132
- [13] Kim D A, Lee J S, Park M B, et al. Effect of etching and aging conditions on the structural, chemical and optical characteristics of porous silicon. *J Korean Phys Soc*, 2003, 42: S184